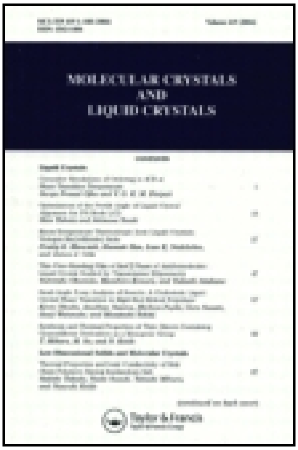

Molecular Crystals and Liquid Crystals Science and Technology. Section A. Molecular Crystals and Liquid Crystals

Publication details, including instructions for authors and subscription information:
http://www.tandfonline.com/loi/gmcl19

Electrochemical Reduction of $Ag_4Hf_3S_8$ in a Nonaqueous Lithium Cell

Hiroaki Wada [a] & Kenji Sakamaki [a] [b]

[a] National Institute for Research in Inorganic Materials (NIRIM), 1-1 Namiki, Tsukuba, Ibaraki, 305-0044, Japan

[b] Japan Science and Technology Corporation (JST)

Version of record first published: 24 Sep 2006

To cite this article: Hiroaki Wada & Kenji Sakamaki (2000): Electrochemical Reduction of $Ag_4Hf_3S_8$ in a Nonaqueous Lithium Cell, Molecular Crystals and Liquid Crystals Science and Technology. Section A. Molecular Crystals and Liquid Crystals, 340:1, 89-94

To link to this article: http://dx.doi.org/10.1080/10587250008025448

Mol. Cryst. and Liq. Cryst., 2000, Vol. 340, pp. 89-94
Reprints available directly from the publisher
Photocopying permitted by license only

Electrochemical Reduction of $Ag_4Hf_3S_8$ in a Nonaqueous Lithium Cell

HIROAKI WADA[a]* and KENJI SAKAMAKI[ab]

[a]*National Institute for Research in Inorganic Materials (NIRIM), 1–1 Namiki, Tsukuba, Ibaraki 305–0044, Japan and* [b]*Japan Science and Technology Corporation (JST)*

A basic nature of cubic $Ag_4Hf_3S_8$ for electrochemical Li insertion was examined with relation to cell properties and Rietveld analyses for *ex-situ* X-ray powder diffraction patterns observed at several discharge steps. The composition dependence of cell voltage curves observed in the closed type Li/1M-$LiPF_6$ in PC/$Ag_4Hf_3S_8$ cell showed a long plateau at around 2.2–2.0 V up to $Li_xAg_4Hf_3S_8$ ($x \le 3$). The cell voltage decreased with an increase of Li intercalation and final lithiated phase was assigned to cubic $Li_xAg_yHf_3S_8$ ($x > 3$, $x + y = 7$). The electrochemical lithiation of $Ag_4Hf_3S_8$ at low constant current densities proceeded topochemically. The structures of lithiated phases were solved without changing the space group $P4_332$ (No. 212) for $Ag_4Hf_3S_8$ host, indicating that Hf_3S_8 framework structure was kept through the lithiation.

Keywords: ternary silver sulfide; $Ag_4Hf_3S_8$; argyrodite phase; lithium cell

INTRODUCTION

Ternary silver sulfides with general formula $Ag_\alpha M_\beta S_\gamma$ ($\alpha + n\beta = 2\gamma$, $\alpha \ge \beta$, and $\gamma = 8$) are of particularly interest in that these compounds exhibit relatively high Ag ionic conductivity and have a common structural feature which is called the "argyrodite family" phase designated by Kuhs *et al.*[1]. Wada *et al.* have extended the preparative studies on ternary silver sulfides containing the transition metal of the group 4 and 5 also found several new compounds with higher Ag ionic conductivity [2-5]. One of them, $Ag_4Hf_3S_8$ crystallizes in the

---

* Corresponding author, wadah@nirim.go.jp

cubic system and has a three-dimensional rigid framework structure [4], which led to the lithiation of $Ag_4Hf_3S_8$ toward the application for lithium cell and the formation of superionic or fast ionic conductor. Although high temperature solid state procedures failed to produce the quaternary compounds $Li_xAg_yHf_3S_8$, preparation by room temperature soft chemical intercalation method using *n*-butyl lithium proved successful [6].

In this paper we report on the cathodic properties of $Ag_4Hf_3S_8$ in room temperature organic electrolyte lithium ion cell, $Li/Li^+/Ag_4Hf_3S_8$. Structural properties for electrochemical lithium intercalation will be discussed on the basis of their cell properties and Rietveld analyses for *ex-situ* X-ray powder diffraction (XRD) patterns observed at several discharge steps.

EXPERIMENTAL

The details of sample preparation were described in the previous papers [3-6]. Compact $Ag_4Hf_3S_8$ pellets were used as cathode after annealing them at 200°C for two days in a sealed evacuated quartz tube. A closed type cell which is made of Teflon was used in order to adopt any organic solvents and protect the cell against moisture inside the argon box. Cell properties were measured with battery charge/discharge unit (HJR-110mSM6, Hokuto Denko) at several low constant current densities in order to obtain near-equilibrium data.

RESULTS AND DISCUSSION

To gain a basic nature of $Ag_4Hf_3S_8$ for electrochemical Li insertion, cathode material consists of only $Ag_4Hf_3S_8$ without conductive mixture and binder even though the cell shows poor performance.

Preliminary experiments show that cell voltage and discharge curve profiles of $Li/Li^+/Ag_4Hf_3S_8$ depend on the Li-ion conduction electrolyte. Although molar conductivity in propylene carbonate (PC) does not change between $LiPF_6$ (5.8 $S{\cdot}cm^2$) and $LiClO_4$ (5.6 $S{\cdot}cm^2$)[7], $LiPF_6$ is better than $LiClO_4$ in this system. ICP-AES results for lithiated samples show that the mole ratios of Li against Hf range from 0.23 to 1.74, indicating that the maximum 5.3 mole Li could be incorporated into the $Ag_4Hf_3S_8$ host. No native Ag peaks were observed in XRD patterns up to the incorporation of about 3 mole Li into $Ag_4Hf_3S_8$. After cycling the cell, deposition products on Li anode were qualitatively analyzed by DC arc AES. No elements of constituent parts of $Ag_4Hf_3S_8$ were detected.

Using the closed type cell, the cathodic properties of $Ag_4Hf_3S_8$ were carefully examined. Figure 1 shows the first discharge curves in Li/1M-$LiPF_6$ in PC /$Ag_4Hf_3S_8$ at various current densities. The composition ratio of Li against $Ag_4Hf_3S_8$ was determined coulometrically. At low current density the time taken to reach the final discharge voltage up to 1 V was more than one month. Unfortunately cell reaction for 52 μA/cm^2 discharge process stopped at 2.14 V by power supply interruption for building repair as indicated by an arrow in Fig. 1. Although the cell potential decreased with an increase of discharge current density, discharge curve profiles were the same below 130 μA/cm^2. The initial cell voltage was found to be in excess of 3 V. For low current densities the discharge curves can be classified into three parts such as (1) initial state to the onset of plateau region, (2) a long plateau at around 2.2-2.0 V, and (3) below 1.9 V region. At relatively high current density of 260 μA/cm^2 cell voltage was decreased steeply.

Figure 2 shows XRD patterns of cathodes observed at the several different cut-off voltages against the starting cubic $Ag_4Hf_3S_8$ with lattice constant of *a* = 10.905 Å [4]. The XRD pattern of current density of 52 μA/cm^2 was observed after discharging up to 2.14 V. For both 130 and 260 μA/cm^2 discharge processes XRD patterns were taken after reaching at 1 V. Rietveld analyses of

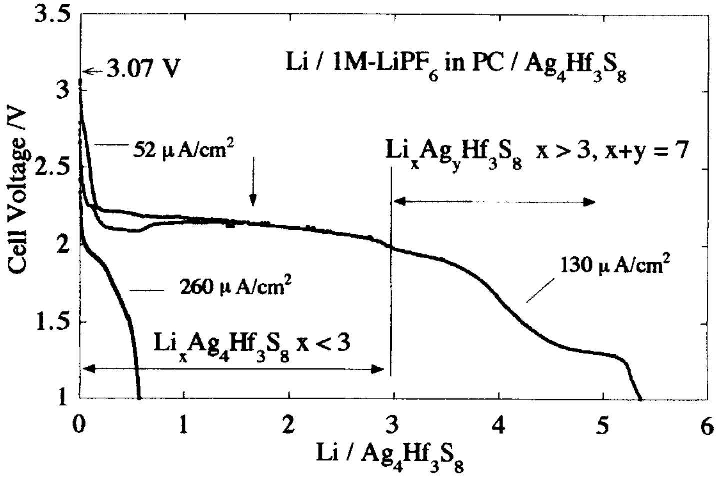

FIGURE 1 Discharge properties for Li/1M-$LiPF_6$ in PC/$Ag_4Hf_3S_8$ cell as a function of current density.

these patterns suggest coexistence of three phases, that is, lithiated phase, original $Ag_4Hf_3S_8$, and Ag. These XRD patterns were observed after grinding the lithiated sample removed from current collector so that conductive Ag paste was incorporated into the sample. The presence of original $Ag_4Hf_3S_8$ phase is considered as unreacted $Ag_4Hf_3S_8$. For 52 μA/cm² the presence of $Ag_4Hf_3S_8$ is reasonable because cell reaction was stopped at the intermediate cell voltage, 2.14 V, within the long plateau region. At higher current density of 260 μA/cm² cell reaction might not proceed equilibrium situation due to a low migration rate of intercalated Li in $Ag_4Hf_3S_8$. Mass fractions of unreacted $Ag_4Hf_3S_8$ in the above cases were approximately 40-45 wt% which was determined by Rietveld multi-phase analyses [8]. The composition ratio of Li against $Ag_4Hf_3S_8$ as shown in Fig. 1 suggests an averaged value. These lithiation reactions proceed not homogeneously but from the surface region. The XRD pattern observed after discharging up to 1 V with the current density of 130 μA/cm² showed that almost all $Ag_4Hf_3S_8$ became to lithiated phase.

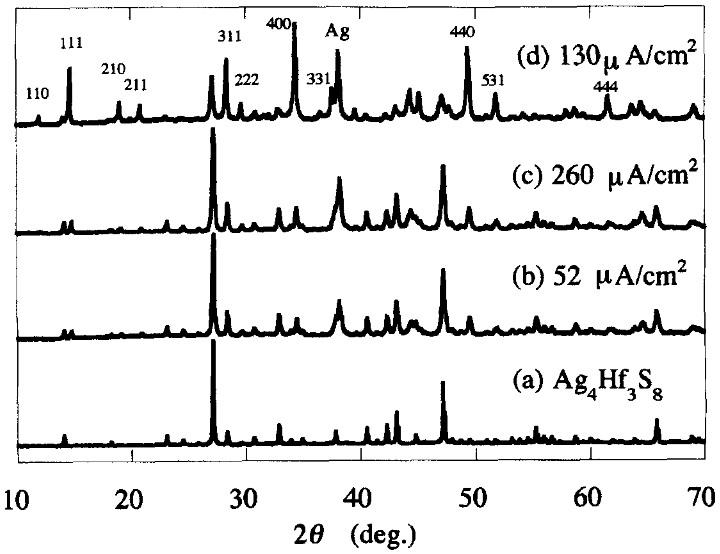

FIGURE 2 XRD patterns of $Ag_4Hf_3S_8$ cathode after discharging up to 2.14 V with 52 μA/cm² (b), 1.0 V with 260 μA/cm² (c), 1.0 V with 130 μA/cm² (d) with reference to the original $Ag_4Hf_3S_8$ (a).

Suitable models for a way of lithiation of $Ag_4Hf_3S_8$ are proposed under the requirements of total charge balance and occupation sites for Li. If the Li atoms reside in octahedral sites, the maximum lithiated product is to be $Li_3Ag_4Hf_3S_8$ and formal valence of all Hf is reduced from +4 to +3 (Model A). If the Li atoms reside in tetrahedral sites, the maximum lithiated product is to be $Li_6Ag_4Hf_3S_8$ in which formal valence of all Hf must be reduced from +4 to +2 (Model B-1). Although the number of tetrahedral sites are enough to satisfy Model B-1 condition, Hf_3S_8 structure may be destroyed by the reduction of all Hf atoms from +4 to +2. Therefore, $Li_3Ag_4Hf_3S_8$ is proper for the tetrahedral occupation of Li (Model B-2). When Li atoms more than three mole intercalate into $Ag_4Hf_3S_8$, a formation of $Li_xAg_yHf_3S_8$ ($x > 3$, $x + y = 7$) is expected. In such the case ion exchange occurs between Ag^+ and Li^+ and some Ag move out from the mother structure. In the range of Li content of $3 < x \leq 7$, lithium atoms occupy only in tetrahedral sites (Model C-1) or in both tetrahedral and octahedral sites (Model C-2).

XRD Rietveld analyses [8] for the electrochemically lithiated samples were performed based on the above mentioned models. All data could be solved without changing the space group $P4_332$ (No. 212) for $Ag_4Hf_3S_8$ host, indicating that Hf_3S_8 framework structure was kept through the lithiation. Thus the lithiated phase pattern could be assigned to cubic lithiated-$Ag_4Hf_3S_8$, which was essentially identical to that of chemically lithiated $Ag_4Hf_3S_8$ by *n*-BuLi treatment [6]. Refined lattice constants for electrochemically lithiated phase range from 10.435 to 10.411 Å, which are a little bit smaller than that of starting cubic $Ag_4Hf_3S_8$ (10.905 Å). The vacancy sites became smaller due to the intercalation of Li so that Hf_3S_8 framework structure might be compact.

On the basis of discharge properties, ICP-AES chemical analyses, and XRD Rietveld analyses, the electrochemical lithiation of $Ag_4Hf_3S_8$ is considered as following. For lower Li intercalated $Ag_4Hf_3S_8$, the lithiated phase could be assigned to cubic $Li_xAg_4Hf_3S_8$ ($x \leq 3$). But the final conventional reliability factors obtained by Rietveld analyses were not so serious difference in between Model A and B-2. As shown in Fig. 1, cell voltage shows the long plateau at around 2.2-2.0 V up to the intercalation of 3 mole Li into $Ag_4Hf_3S_8$. The XRD pattern observed after 130 $\mu A/cm^2$ discharge up to 1 V (Fig. 2(d)) could be solved by Model C. The present XRD data do not indicate the site preference of whether Li atoms reside on tetrahedral or octahedral vacancies.

When the formation of cubic $Li_xAg_yHf_3S_8$ ($x > 3$, $x + y = 7$) was initiated by further incorporation of Li atoms, the cell voltage decreased with an increase of Li intercalation as shown in Fig. 1.

CONCLUSION

The electrochemical lithiation of $Ag_4Hf_3S_8$ at low constant current densities proceeded topochemically. The structures of lithiated phases were determined without changing the space group $P4_332$ (No. 212) for $Ag_4Hf_3S_8$ host, indicating that Hf_3S_8 framework structure was stable during the electrochemical lithiation. The cell voltage showed the long plateau at around 2.2-2.0 V up to the intercalation of 3 mole Li into $Ag_4Hf_3S_8$. The lithiated phase was assigned to cubic $Li_xAg_4Hf_3S_8$ ($x \leq 3$). Further insertion of Li into cubic $Li_xAg_4Hf_3S_8$ ($x \leq 3$) led to the decrease of cell voltage. Final lithiated phase was assigned to cubic $Li_xAg_yHf_3S_8$ ($x > 3$, $x + y = 7$), which was essentially identical to that of chemically lithiated $Ag_4Hf_3S_8$ by *n*-BuLi treatment [6].

Acknowledgments

We thank the NIRIM technical supporting staffs, Y. Yajima, S. Takenouchi, A. Sato, K. Kosuda, and T. Wada for their precise instrumental set up and analyses.

References

[1] W. F. Kuhs, R. Nitsche, and K. Scheunemann, *Mat. Res. Bull.*, **14**, 241 (1979).
[2] H. Wada and M. Onoda, *J. Less-Common Metals*, **175**, 209 (1991).
[3] H. Wada, O. Amiel, and A. Sato, *J. Alloys Compounds*, 219, **55** (1995).
[4] O. Amiel and H. Wada, *J. Solid State Chem.*, **115**, 112 (1995).
[5] H. Wada, O. Amiel, and A. Sato, *Solid State Ionics*, **79**, 129 (1995).
[6] H. Wada, O. Amiel, and S. Takenouchi, *Solid State Ionics*, **113**, 487 (1998).
[7] M. Ue and S. Mori, *J. Electrochem. Soc.*, **142**, 2577 (1995).
[8] F. Izumi, in *The Rietveld method*, edited by R. A. Young, (Oxford University Press, Oxford, 1993), Chap 13, p. 236.